

MIT Open Access Articles

*Have Aerosols Caused the Observed
Atlantic Multidecadal Variability?*

The MIT Faculty has made this article openly available. **Please share** how this access benefits you. Your story matters.

Citation: Zhang, Rong, Thomas L. Delworth, Rowan Sutton, Daniel L. R. Hodson, Keith W. Dixon, Isaac M. Held, Yochanan Kushnir, et al. "Have Aerosols Caused the Observed Atlantic Multidecadal Variability?" *Journal of the Atmospheric Sciences* 70, no. 4 (April 2013): 1135-1144. © 2013 American Meteorological Society

As Published: <http://dx.doi.org/10.1175/JAS-D-12-0331.1>

Publisher: American Meteorological Society

Persistent URL: <http://hdl.handle.net/1721.1/81289>

Version: Final published version: final published article, as it appeared in a journal, conference proceedings, or other formally published context

Terms of Use: Article is made available in accordance with the publisher's policy and may be subject to US copyright law. Please refer to the publisher's site for terms of use.



Have Aerosols Caused the Observed Atlantic Multidecadal Variability?

RONG ZHANG,* THOMAS L. DELWORTH,* ROWAN SUTTON,+ DANIEL L. R. HODSON,+ KEITH W. DIXON,* ISAAC M. HELD,* YOCHANAN KUSHNIR,# JOHN MARSHALL,@ YI MING,* RYM MSADEK,* JON ROBSON,+ ANTHONY J. ROSATI,* MINGFANG TING,# AND GABRIEL A. VECCHI*

* NOAA/Geophysical Fluid Dynamics Laboratory, Princeton, New Jersey

+ National Centre for Atmospheric Science—Climate, Department of Meteorology, University of Reading, Reading, United Kingdom

Lamont-Doherty Earth Observatory, Columbia University, Palisades, New York

@ Department of Earth, Atmospheric and Planetary Sciences, Massachusetts Institute of Technology, Cambridge, Massachusetts

(Manuscript received 30 November 2012, in final form 18 December 2012)

ABSTRACT

Identifying the prime drivers of the twentieth-century multidecadal variability in the Atlantic Ocean is crucial for predicting how the Atlantic will evolve in the coming decades and the resulting broad impacts on weather and precipitation patterns around the globe. Recently, Booth et al. showed that the Hadley Centre Global Environmental Model, version 2, Earth system configuration (HadGEM2-ES) closely reproduces the observed multidecadal variations of area-averaged North Atlantic sea surface temperature in the twentieth century. The multidecadal variations simulated in HadGEM2-ES are primarily driven by aerosol indirect effects that modify net surface shortwave radiation. On the basis of these results, Booth et al. concluded that aerosols are a prime driver of twentieth-century North Atlantic climate variability. However, here it is shown that there are major discrepancies between the HadGEM2-ES simulations and observations in the North Atlantic upper-ocean heat content, in the spatial pattern of multidecadal SST changes within and outside the North Atlantic, and in the subpolar North Atlantic sea surface salinity. These discrepancies may be strongly influenced by, and indeed in large part caused by, aerosol effects. It is also shown that the aerosol effects simulated in HadGEM2-ES cannot account for the observed anticorrelation between detrended multidecadal surface and subsurface temperature variations in the tropical North Atlantic. These discrepancies cast considerable doubt on the claim that aerosol forcing drives the bulk of this multidecadal variability.

1. Introduction

The observed twentieth-century multidecadal variations of area-averaged North Atlantic sea surface temperature (NASST) exhibit significant regional and hemispheric climate associations (Enfield et al. 2001; Sutton and Hodson 2005; Knight et al. 2006; Zhang and Delworth 2006; Zhang et al. 2007; Kushnir and Stein 2010; Ting et al. 2011; Sutton and Dong 2012). These variations are highly correlated with the multidecadal variations of the tropical North Atlantic SST and Atlantic hurricane activity (Goldenberg et al. 2001; Knight et al. 2006; Zhang and Delworth 2006). In particular, tropical North Atlantic surface warming coincided with above-normal Atlantic hurricane activity during the

1950s, 1960s, and the recent decade. These multidecadal NASST variations are often thought to be associated with Atlantic meridional overturning circulation (AMOC) variability (Delworth and Mann 2000; Latif et al. 2004; Knight et al. 2005). On the other hand, some authors have suggested that they are at least in part driven by changes in the radiative forcing (Mann and Emanuel 2006; Villarini and Vecchi 2013). Various approaches have been proposed for quantitative attribution of NASST variations to a radiatively forced part and a part arising from AMOC variability (Kravtsov and Spannagle 2008; Ting et al. 2009; Zhang and Delworth 2009; DelSole et al. 2011; Wu et al. 2011; Terray 2012), and they show consistently that the role of internal variability cannot be ignored in multidecadal NASST variations.

Recently, Booth et al. (2012, hereafter B12) showed that the Hadley Centre Global Environmental Model, version 2, Earth system configuration (HadGEM2-ES;

Corresponding author address: Rong Zhang, NOAA/GFDL, 201 Forrester Rd., Route 1, Princeton, NJ 08540.
E-mail: rong.zhang@noaa.gov

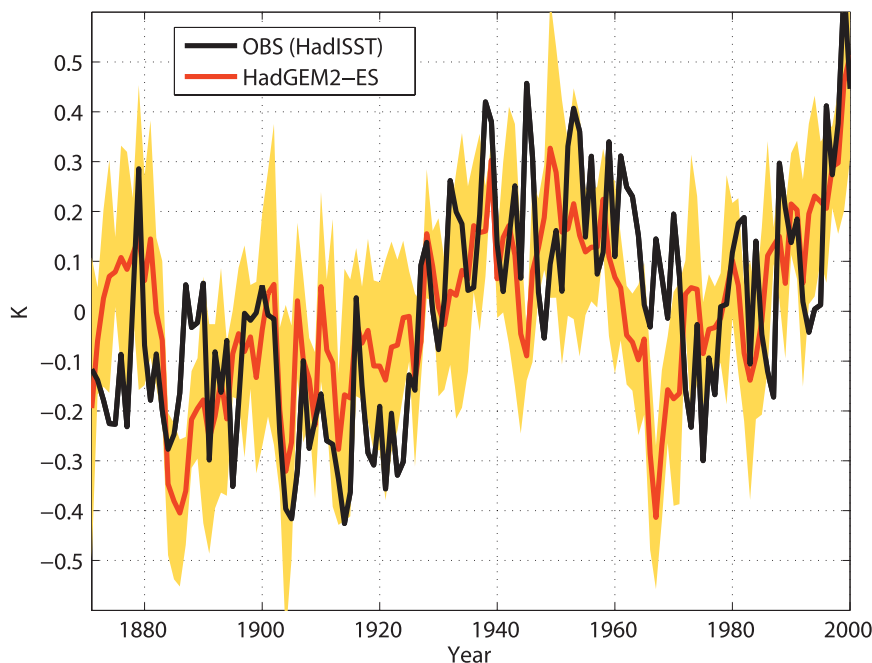


FIG. 1. Area-averaged NASST anomaly (0° – 60° N, 75° – 7.5° W), adapted from Fig. 1b in B12. Orange line: ensemble mean of HadGEM2-ES historical simulations with all external forcing (all forcings). Black line: observations (HadISST). Yellow shading: 1 std dev of ensemble spread of HadGEM2-ES all forcings. All anomalies are relative to 1871–2000 mean.

Jones et al. 2011) closely reproduces the amplitude and phase of the observed multidecadal variations of area-averaged NASST, especially over the second half of the twentieth century (Fig. 1). The multidecadal variations simulated in HadGEM2-ES are primarily driven by aerosol indirect effects that modify net surface short-wave radiation. On the basis of these results, B12 concluded that aerosols are a primary source of this multidecadal variability. However, B12 mainly compared the evolution of modeled and observed area-averaged NASST. In this study we show that there are major discrepancies between the HadGEM2-ES simulations and many observed changes in the North Atlantic. The discrepancies cast doubt upon the main conclusion of B12.

In section 2, the analysis methods and data used in this study are described. In sections 3–6 we compare the HadGEM2-ES simulations with observations over a range of variables. The purpose of these comparisons is to assess more completely how well the HadGEM2-ES simulations actually replicate the observed evolution of the North Atlantic over the twentieth century. In section 3 we examine North Atlantic upper-ocean heat content. In section 4 we examine the spatial pattern of multidecadal SST changes. In section 5 we examine sea surface salinity (SSS) in the North Atlantic. In section 6 we examine subsurface temperature anomalies in the

tropical North Atlantic (TNA). Our conclusions are presented in section 7.

2. Description of method and data

In this study, the observed upper-ocean heat content is derived from a yearly averaged dataset of objectively analyzed ocean temperature anomalies since 1955 (Levitus et al. 2009). The observed SSS data are from the pentadally averaged dataset of objectively analyzed ocean salinity anomalies since 1957 (Boyer et al. 2005). The observed SST is based on the Hadley Centre Sea Ice and Sea Surface Temperature dataset (HADISST) since 1871 (Rayner et al. 2003). The ensemble of four HadGEM2-ES historical simulations with all external forcing (“all forcings”) used in B12 are downloaded from phase 5 of the Coupled Model Intercomparison Project (CMIP5) model output archive at <http://esgf-index1.ceda.ac.uk/esgf-web-fe/>. The ensemble of three “constant aerosols” HadGEM2-ES historical simulations (same as the first three members of the all-forcings simulation except that anthropogenic aerosol emissions are fixed at 1860 levels) was provided to us by B. Booth and P. Halloran from the Met Office Hadley Centre (MOHC). We assume linearity in the sense that the ensemble mean difference (first three members) between all-forcings and constant-aerosols HadGEM2-ES

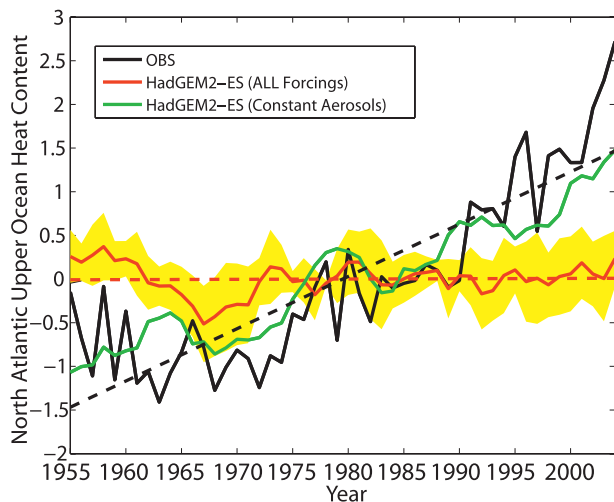


FIG. 2. North Atlantic upper-ocean heat content anomaly. Red line: area-averaged North Atlantic upper-ocean heat content anomaly ($\times 10^{22}$ J) (0–700 m; 0° – 60° N, 75° – 7.5° W) from ensemble mean of HadGEM2-ES all-forcings simulations. Yellow shading: 1 std dev of ensemble spread of all forcings. Green line: ensemble mean from constant-aerosols historical simulations. Black line: observations. All anomalies are relative to 1955–2004 mean. The dashed lines are linear trends for the respective variables. The 1955–2004 trend is 0.599×10^{22} J decade $^{-1}$ for observations and 0.003×10^{22} J decade $^{-1}$ for HadGEM2-ES all-forcings ensemble mean.

historical simulations is assumed to represent the net response to anthropogenic aerosols.

3. North Atlantic upper-ocean heat content

Substantial warming trends in the upper-ocean heat content have been observed in most ocean basins since the middle of the twentieth century (Domingues et al. 2008; Levitus et al. 2009). Gleckler et al. (2012), using multiple observations (Domingues et al. 2008; Ishii and Kimoto 2009; Levitus et al. 2009) and externally forced and unforced simulations from CMIP3, shows that the observed warming trend of upper-ocean heat content in the North Atlantic (and other basins) over the second half of the twentieth century is typically consistent with the response in these CMIP3 models to the sum of all external forcing. The results suggest that changes in anthropogenic forcing (especially increasing greenhouse gases) play an important role in the observed upper-ocean warming trend.

In contrast to the observed heat content increase, the all-forcings HadGEM2-ES historical simulations exhibit no trend in the area-averaged North Atlantic upper-ocean heat content (0–700 m) between 1955 and 2004 (Fig. 2). The observed warming trend (0.599×10^{22} J decade $^{-1}$) for the period of 1955–2004 is clearly

inconsistent with the modeled trend (Fig. 2). Over the same period, the simulated trends for individual all-forcings ensemble members range from a minimum of -0.141×10^{22} J decade $^{-1}$ to a maximum of 0.118×10^{22} J decade $^{-1}$, all much smaller than that observed. The HadGEM2-ES all-forcings simulations, which have strong aerosol effects, suggest that there is no net radiatively forced warming in the North Atlantic upper ocean over the second half of the twentieth century.

Using a different model [Geophysical Fluid Dynamics Laboratory Climate Model, version 2.1 (GFDL CM2.1)], Delworth et al. (2005) showed that the surface waters cooled by aerosol effects can penetrate into the subsurface ocean through subduction, and persist in the subsurface for decades, thereby offsetting subsequent greenhouse gas induced subsurface warming. The cooled surface waters can reduce vertical stratification in the ocean thus have higher subduction rates (Marshall and Nurser 1992). In HadGEM2-ES, over the second half of the twentieth century, the simulated subsurface aerosol-induced cooling is evidently so strong that it counteracted the subsurface greenhouse gas-induced warming, resulting in a net subsurface cooling in the North Atlantic. The subsurface cooling lags the surface response by decades and even persists into the 1990s (not shown). On the contrary, in observations the subsurface temperature is dominated by warm anomalies over this period (Domingues et al. 2008; Ishii and Kimoto 2009; Levitus et al. 2009).

In the ensemble mean of the all-forcings HadGEM2-ES simulations, the simulated subsurface cooling trend offsets the surface warming trend, so there is almost no net heat content change integrated over the North Atlantic upper ocean (0–700 m) for the second half of the twentieth century. In contrast, the ensemble of constant aerosols HadGEM2-ES historical simulations shows a clear warming trend in the North Atlantic upper-ocean heat content (Fig. 2). In B12, the constant aerosols simulations are compared with all-forcings simulations to demonstrate the important role of anthropogenic aerosols in NASST. Here the comparison between these two sets of simulations also shows the important role of anthropogenic aerosols in causing the discrepancy between simulated and observed trends in the North Atlantic upper-ocean heat content. This discrepancy with observations suggests that the aerosol effects are strongly overestimated over the North Atlantic in HadGEM2-ES.

4. Spatial pattern of multidecadal SST changes

The pattern of SST changes associated with the prominent cooling of NASST that occurred in the late 1960s and 1970s is distinctly different in the HadGEM2-ES

all-forcings simulations from that seen in observations, both within and outside the North Atlantic (Figs. 3a,b). The observed cooling is most pronounced in the subpolar and midlatitude North Atlantic, while the model shows a more extensive cooling in the tropical North Atlantic than seen in observations. The observed abrupt cooling in the early 1970s has the largest amplitude in the subpolar North Atlantic (Thompson et al. 2010) and coincided with a rapid freshening of the subpolar North Atlantic referred to as the “great salinity anomaly” (Dickson et al. 1988). This observed cooling in the subpolar North Atlantic is largely underestimated in HadGEM2-ES all-forcings simulations.

Outside the North Atlantic, the HadGEM2-ES all-forcings simulations show excessive cooling in the Barents Sea, North Pacific, tropical South Atlantic, Indian Ocean, and Southern Ocean in comparison with that observed (Figs. 3a,b). The net response to anthropogenic aerosols (Fig. 3c, difference between all forcings and constant aerosols) is multidecadal cooling in most ocean basins. In contrast, the observed multidecadal SST changes are characterized by a dipole pattern in the Atlantic, suggestive of an important role for variations in the AMOC and related variations in Atlantic heat transport (Zhang and Delworth 2005; Ting et al. 2009; Robson et al. 2012).

This discrepancy is also reflected in the 10-yr low-pass filtered time series of SST anomalies averaged over the North Atlantic versus those averaged over the rest of the World Ocean (Fig. 4). In observations, the low-pass filtered North Atlantic SST anomaly is characterized by a pronounced multidecadal variability, whereas the low-pass filtered SST anomaly averaged over the rest of the World Ocean is dominated by an increasing trend with much weaker multidecadal variability (Fig. 4a). In particular, for the period of 1961–80, although the observed North Atlantic SST was colder than the previous period of 1941–60, the observed SST averaged over the rest of the World Ocean did not exhibit a cooling (Fig. 4a). However, in the HadGEM2-ES all-forcings simulations, the low-pass filtered SST anomaly averaged over the rest of the World Ocean shows a strong multidecadal variability, and the abrupt post-1960 cooling simulated in the North Atlantic SST is also present in the SST averaged over the rest of the World Ocean (Fig. 4b). Although the simulated low-pass filtered North Atlantic SST anomaly resembles the observations (Fig. 4c), the simulated low-pass filtered SST anomaly averaged over the rest of the World Ocean is quite different from the observations (Fig. 4d). The observed low-pass filtered SST anomaly averaged over the rest of the World Ocean is outside the simulated ensemble spread for most of the twentieth century (Fig. 4d). The results consistently suggest that the time-varying aerosols in HadGEM2-ES

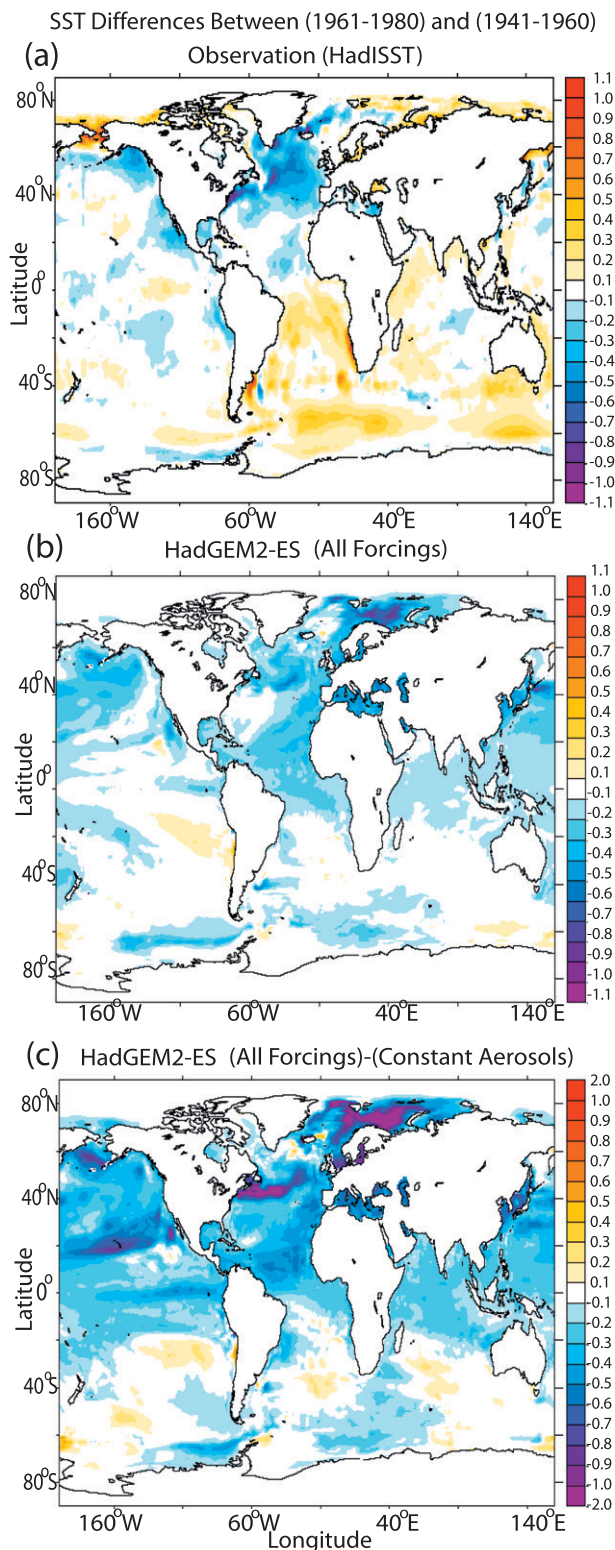


FIG. 3. SST differences (K) between the North Atlantic cold period (1961–80) and the North Atlantic warm period (1941–60). (a) Observations, (b) HadGEM2-ES all-forcings ensemble mean, and (c) ensemble mean difference between HadGEM2-ES all forcings and constant aerosols.

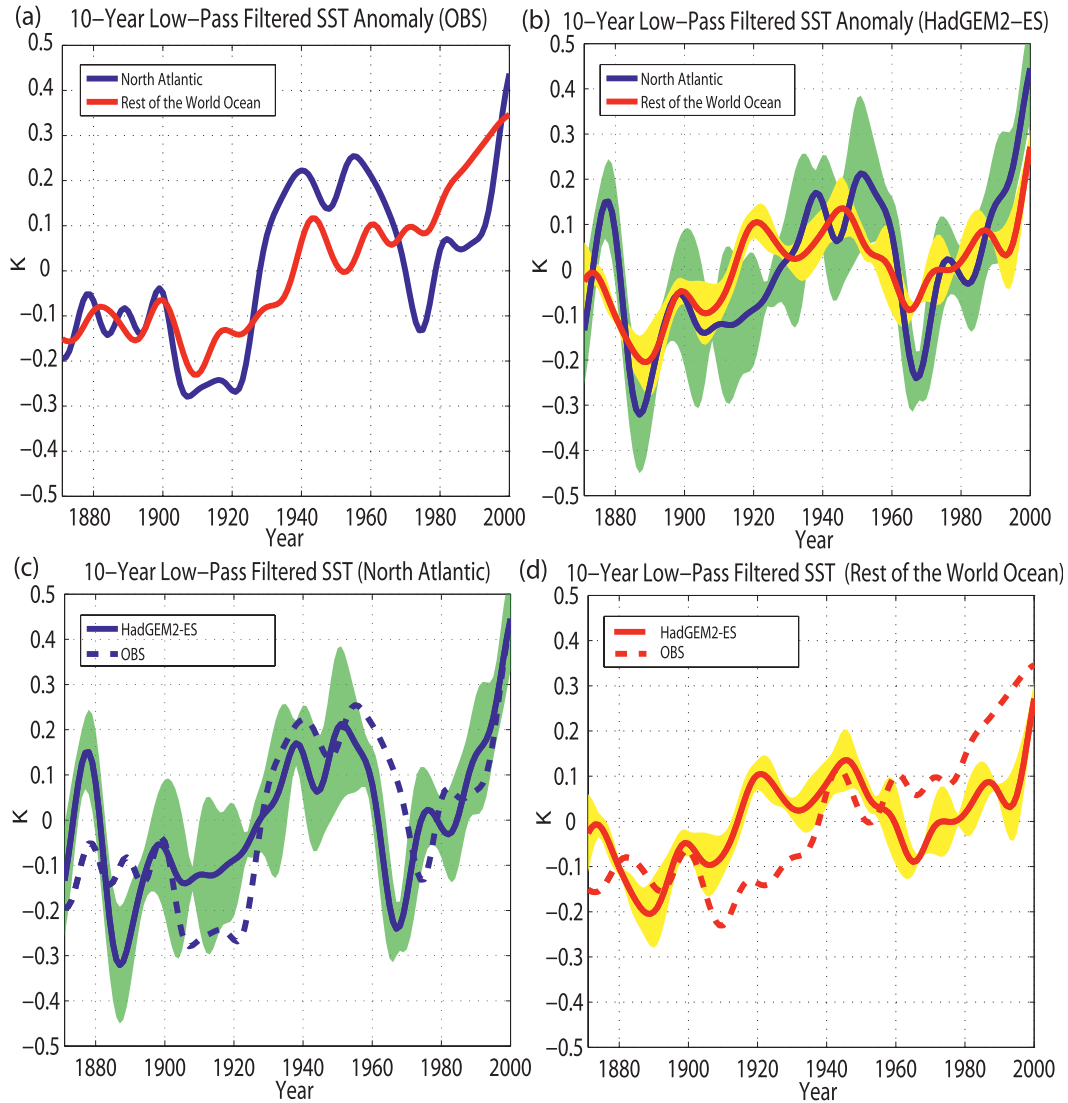


FIG. 4. Comparison of 10-yr low-pass filtered NASST anomaly (blue) with 10-yr low-pass filtered SST anomaly averaged for the rest of the World Ocean (red). (a) Observations (HadISST). (b) Ensemble mean of HadGEM2-ES all forcings. Green shading: 1 std dev of ensemble spread for low-pass filtered NASST anomaly; yellow shading: 1 std dev of ensemble spread for low-pass filtered SST anomaly averaged for the rest of the World Ocean. (c) Low-pass filtered NASST anomaly from HadGEM2-ES all forcings (blue solid line) and observations (blue dashed line). (d) Low-pass filtered SST anomaly averaged for the rest of the World Ocean from HadGEM2-ES all forcings (red solid line) and observations (red dashed line). The color shadings in (c) and (d) are as in (b).

all-forcings simulations induce an unrealistic global-scale multidecadal variability.

5. Subpolar North Atlantic sea surface salinity anomalies

The simulation of the subpolar North Atlantic SSS in the HadGEM2-ES all-forcings simulations also shows important differences to observations. In observations the subpolar North Atlantic SSS anomalies exhibit

multidecadal variations that are coherent and in phase with variations in basin-mean and subpolar NASST (Fig. 5), with no long-term trend. In contrast, the subpolar North Atlantic SSS simulated in HadGEM2-ES shows a salinification trend, as well as variations that are largely out of phase with the observed subpolar NA SSS and also out of phase with the simulated basin-mean NASST variations over the second half of the twentieth century (Figs. 5 and 4c). The simulated salinification trend in the subpolar North Atlantic is consistent with

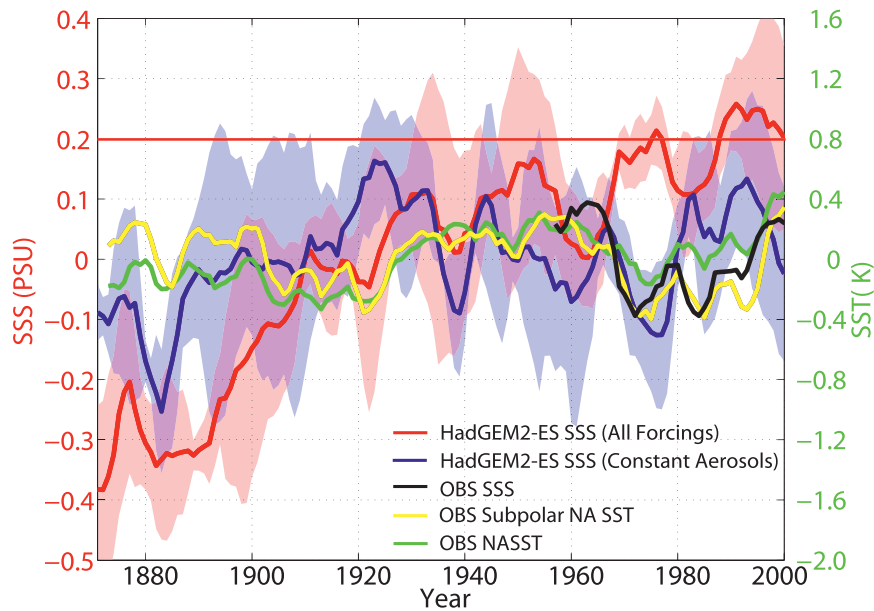


FIG. 5. Subpolar North Atlantic SSS anomaly (50° – 65° N, 60° W– 0°). Red line: subpolar North Atlantic SSS anomaly from ensemble mean of HadGEM2-ES all-forcings simulations. Blue line: subpolar North Atlantic SSS anomaly from ensemble mean of HadGEM2-ES constant aerosols simulation. Black line: observed subpolar North Atlantic SSS anomaly, relative to the 1957–2000 mean. Yellow line: observed subpolar North Atlantic SST anomaly, relative to the 1871–2000 mean. Green line: observed basin-averaged NASST anomaly, relative to the 1873–2000 mean. Thin red line: the 0.2-psu difference in the climatological mean subpolar North Atlantic SSS over the entire period 1873–2000 between HadGEM2-ES all forcings and constant aerosols. All anomalies are pentadally averaged.

the response to aerosol forcing as shown in a previous study using GFDL CM2.1 (Delworth and Dixon 2006). The constant aerosols ensemble shows no significant salinification trend at the surface in the subpolar North Atlantic (Fig. 5), and the mean value of subpolar North Atlantic SSS over the period 1871–2000 is 0.2 psu lower in constant aerosols simulations than that in all-forcings simulations, which is consistent with this interpretation.

The subpolar SSS changes are directly linked to changes in deep water formation and large-scale ocean circulation (Curry et al. 1998). The discrepancies in subpolar North Atlantic SSS again suggest the aerosol effects are strongly overestimated in HadGEM2-ES. In contrast, the observed coherent relationships between subpolar North Atlantic SSS/SST and basin-mean NASST variations are consistent with the notion that the AMOC plays an important role in the Atlantic multidecadal variability, as suggested by a number of climate model based studies (Delworth et al. 1997; Robson et al. 2012).

6. Detrended tropical North Atlantic subsurface temperature anomalies

Zhang (2007) showed that the observed multidecadal variations of TNA SST are strongly anticorrelated with

those of TNA subsurface ocean temperature, with long-term trends removed. Therefore, mechanisms that are proposed to explain the observed multidecadal TNA SST variations should also be consistent with the observed anticorrelations between TNA surface and subsurface temperature variations. Further, we note that model results in Zhang (2007) suggest that this out-of-phase relationship between surface and subsurface ocean temperature in the tropical North Atlantic is a distinctive feature of AMOC variations.

Here we apply the same analyses as in Zhang (2007) to the linear detrended TNA SST anomalies and subsurface temperature anomalies from the HadGEM2-ES all-forcings ensemble. The analyses here are not aimed at the question of whether aerosol effects have been overestimated in the HadGEM2-ES, and thus are different from the other discrepancies discussed in sections 3–5. The analyses in this section are to test the hypothesis that the aerosol mechanism can account for the observed anticorrelation between the detrended TNA surface and subsurface temperature variations. The analyses are compared with the detrended observations and the ensemble of water-hosing experiments using a CMIP3 coupled climate model (GFDL CM2.1; Delworth et al. 2006). In the ensemble of water-hosing experiments,

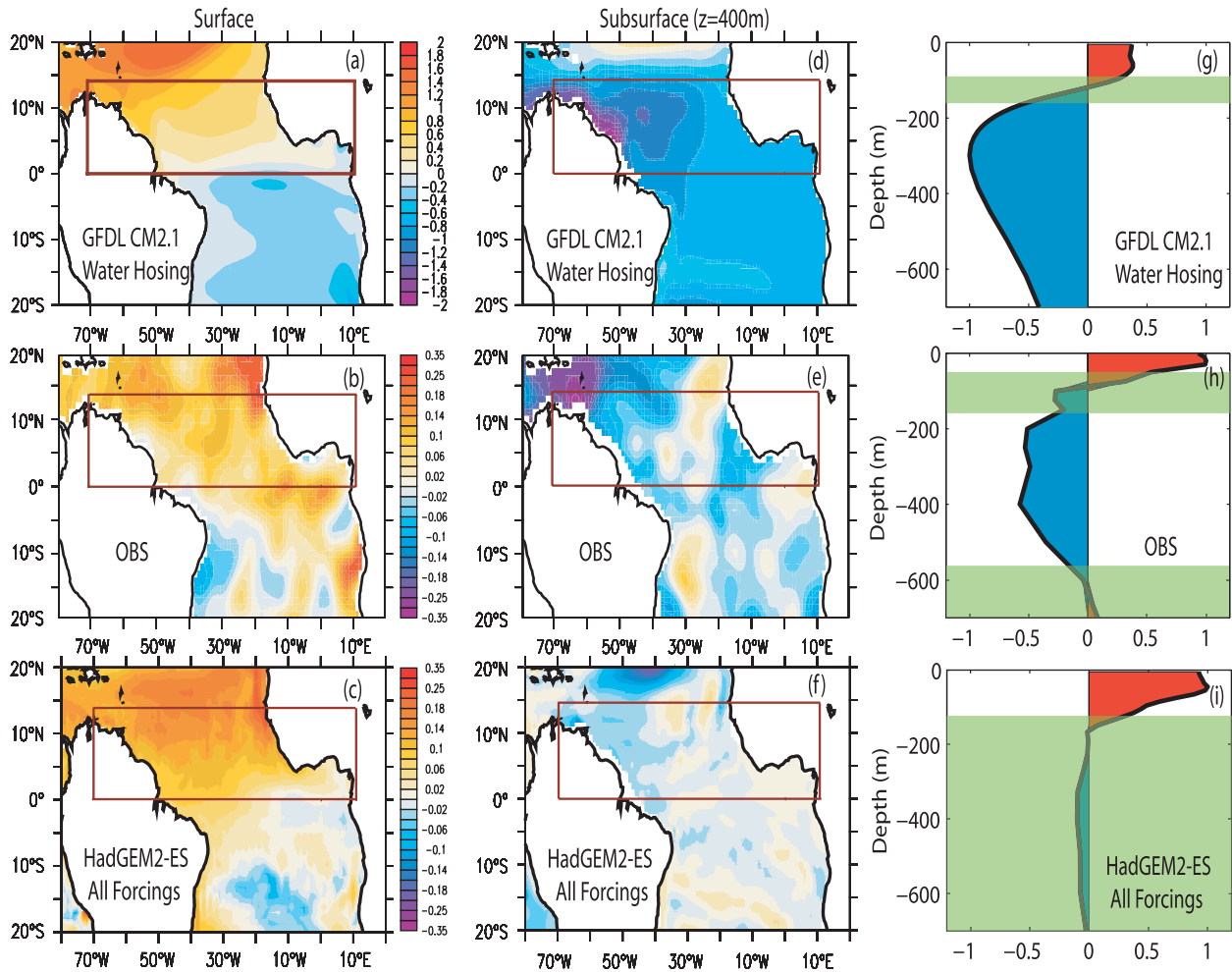


FIG. 6. Regression coefficients of (a)–(c) SST anomaly, (d)–(f) subsurface ocean temperature anomaly ($z = 400\text{ m}$), and (g)–(i) averaged TNA ocean temperature anomaly at different depths onto the time series of the TNA SST anomaly, corresponding to 1 std dev of the TNA SST anomaly. (top) Ensemble mean from water-hosing experiments using GFDL CM2.1, years 1–60. (middle) Low-pass filtered observed data (OBS; 1955–2000). (bottom) Low-pass filtered modeled ensemble mean from HadGEM2-ES all-forcings simulations (1955–2000). The long-term trends have been removed for OBS and HadGEM2-ES. The brown box shows the TNA domain (0° – 14°N , 70°W – 0°) that is used for area average. Panels (g), (h), and (i) are normalized by the maximum absolute value of each regression, respectively, and the green shading covers depths that are not statistically significant at the 90% level of nonzero correlation using the two-tailed Student's t test. Units in (a)–(f) are kelvins.

a strong freshwater flux anomaly is uniformly distributed over the subpolar North Atlantic for 60 years, and the AMOC weakens gradually in response. The changes in TNA temperature (surface and subsurface) in response to the freshwater forcing are indicative of the AMOC effects in the TNA. There is no need for detrending for the ensemble of water-hosing experiments, as all radiative forcings are held constant in this ensemble.

As shown in Zhang (2007), in the water-hosing experiments the AMOC-induced anticorrelated changes between the TNA surface and subsurface temperature are clearly apparent in the spatial regression pattern of

surface and subsurface temperature anomalies onto the TNA SST anomaly (Figs. 6a,d). The detrended observations also show anticorrelated changes—that is, positive regression coefficients over most of the TNA surface and negative regression coefficients over most of the TNA subsurface (Figs. 6b,e). In contrast, the ensemble mean detrended results from the HadGEM2-ES all-forcings simulations show positive regression coefficients over the surface TNA but almost no signals over most of the subsurface TNA (Figs. 6c,f). The vertical structure of the regression of the TNA ocean temperature anomalies onto the TNA SST anomaly (Figs. 6g–i) shows similar results. The TNA SST anomalies

induced by aerosol forcing could slowly diffuse or subduct into the subsurface, but there is no obvious mechanism by which the time-varying aerosol forcing could give rise to subsurface temperature changes of opposite polarity to the SST anomalies on these time scales. Hence, aerosol effects simulated in this all-forcings ensemble cannot account for the anticorrelated multidecadal SST and subsurface temperature variations in the detrended observations for the TNA.

In water-hosing experiments, two dominant processes are excited rapidly by the AMOC weakening—surface southward displacements of the Atlantic ITCZ and subsurface thermocline deepening through the propagation of oceanic waves. These processes act together to produce opposite changes between the TNA surface and subsurface temperature (Zhang 2007). Similar AMOC-induced anticorrelated surface and subsurface TNA variations have also been found in coupled-model simulations with the National Center for Atmospheric Research Community Climate System Model, version 3 (CCSM3; Chiang et al. 2008). A recent study using high-resolution temperature records of the last deglacial transition from a southern Caribbean sediment core also shows that warmer subsurface temperatures correspond to colder surface temperatures and a weaker AMOC during the Younger Dryas (Schmidt et al. 2012). The analyses here suggest that the observed anticorrelated multidecadal TNA SST and subsurface temperature variations are consistent with the mechanism of AMOC variations, and inconsistent with the dominance of changes in aerosols. For example, during the 1970–80s, the observed detrended TNA surface cooling and subsurface warming is consistent with a weaker strength of the AMOC when the Labrador Sea deep water formation was substantially reduced as a result of the Great Salinity Anomaly events (Curry et al. 1998).

We have shown here that out-of-phase temperature variations are seen between the surface and subsurface in the TNA for both observations and in model simulations of AMOC changes. In contrast, this out-of-phase behavior is not seen in the HadGEM2-ES simulations. This suggests that the aerosol mechanism cannot account for the observed anticorrelated multidecadal TNA SST and subsurface temperature variations, regardless of whether the aerosol effects are overestimated. This discrepancy is inconsistent with the interpretation that aerosol forcing drives the bulk of the observed Atlantic multidecadal variability.

7. Conclusions

In this paper we have tried to present a broad, multivariate comparison between the observed changes and

those simulated in the HadGEM2-ES. In this comparison, we have included not only SST in the North Atlantic, but also sea surface salinity and subsurface ocean temperature, as well as the vertical structure of temperature variations.

In summary, key aspects of the HadGEM2-ES simulation exhibit substantial discrepancies with observations. Discrepancies are seen in the North Atlantic upper-ocean heat content, in the spatial pattern of multidecadal SST changes within and outside the North Atlantic, and in the subpolar North Atlantic sea surface salinity. These discrepancies are largely attributable to what appears to be excessively strong aerosol effects. It is also shown that the aerosol effects simulated in the HadGEM2-ES all-forcings ensemble cannot account for the anticorrelated multidecadal SST and subsurface temperature variations of the detrended observations for the tropical North Atlantic.

Anthropogenic and natural aerosols have likely played some role in forcing the observed Atlantic multidecadal variability (Evan et al. 2009; Chang et al. 2011; Villarini and Vecchi 2013), and understanding the magnitude of their influence on the North Atlantic SSTs remains a key challenge. Aerosol indirect effects remain poorly understood owing to difficulties in representing subgrid cloud processes in global climate models (Lohmann et al. 2010). The discrepancies pointed out in this paper call into question the claim of B12 that aerosols have been a dominant forcing of observed Atlantic multidecadal variability and the realism of the HadGEM2-ES simulations of the aerosol influence on North Atlantic SST.

We single out the HadGEM2-ES model for this critique to counterbalance the claims in Booth et al. (2012) for the dominance of aerosol forcing for multidecadal Atlantic variability. Whether it is possible for a model to exhibit comparably large indirect aerosol effects without the inconsistencies with observations outlined here remains to be seen.

Acknowledgments. We acknowledge the World Climate Research Programme's Working Group on Coupled Modelling, which is responsible for CMIP, and we thank the MOHC for producing and making available the HadGEM2-ES all-forcings historical simulations. For CMIP the U.S. Department of Energy's Program for Climate Model Diagnosis and Intercomparison provides coordinating support and led development of software infrastructure in partnership with the Global Organization for Earth System Science Portals. We thank Ben Booth and Paul Halloran from the MOHC for providing us the ensemble of constant aerosols HadGEM2-ES historical simulations.

REFERENCES

- Booth, B. B. B., N. J. Dunstone, P. R. Halloran, T. Andrews, and N. Bellouin, 2012: Aerosols implicated as a prime driver of twentieth-century North Atlantic climate variability. *Nature*, **484**, 228–232.
- Boyer, T. P., S. Levitus, J. I. Antonov, R. A. Locarnini, and H. E. Garcia, 2005: Linear trends in salinity for the World Ocean, 1955–1998. *Geophys. Res. Lett.*, **32**, L01604, doi:10.1029/2004GL021791.
- Chang, C. Y., J. C. H. Chiang, M. F. Wehner, A. R. Friedman, and R. Ruedy, 2011: Sulfate aerosol control of tropical Atlantic climate over the twentieth century. *J. Climate*, **24**, 2540–2555.
- Chiang, J. C. H., W. Cheng, and C. M. Bitz, 2008: Fast teleconnections to the tropical Atlantic sector from Atlantic thermohaline adjustment. *Geophys. Res. Lett.*, **35**, L07704, doi:10.1029/2008GL033292.
- Curry, R. G., M. S. McCartney, and T. M. Joyce, 1998: Oceanic transport of subpolar climate signals to mid-depth subtropical waters. *Nature*, **391**, 575–577.
- DelSole, T., M. K. Tippett, and J. Shukla, 2011: A significant component of enforced multidecadal variability in the recent acceleration of global warming. *J. Climate*, **24**, 909–926.
- Delworth, T. L., and M. E. Mann, 2000: Observed and simulated multidecadal variability in the Northern Hemisphere. *Climate Dyn.*, **16**, 661–676.
- , and K. W. Dixon, 2006: Have anthropogenic aerosols delayed a greenhouse gas-induced weakening of the North Atlantic thermohaline circulation? *Geophys. Res. Lett.*, **33**, L02606, doi:10.1029/2005GL024980.
- , S. Manabe, and R. J. Stouffer, 1997: Multidecadal climate variability in the Greenland Sea and surrounding regions: A coupled model simulation. *Geophys. Res. Lett.*, **24**, 257–260.
- , V. Ramaswamy, and G. Stenchikov, 2005: The impact of aerosols on simulated ocean temperature and heat content in the 20th century. *Geophys. Res. Lett.*, **32**, L24709, doi:10.1029/2005GL024457.
- , and Coauthors, 2006: GFDL's CM2 global coupled climate models. Part I: Formulation and simulation characteristics. *J. Climate*, **19**, 643–674.
- Dickson, R. R., J. Meincke, S. A. Malmber, and A. J. Lee, 1988: The “great salinity anomaly” in the northern North Atlantic 1968–1982. *Prog. Oceanogr.*, **20**, 103–151.
- Domingues, C. M., J. A. Church, N. J. White, P. J. Gleckler, S. E. Wijffels, P. M. Barker, and J. R. Dunn, 2008: Improved estimates of upper-ocean warming and multi-decadal sea-level rise. *Nature*, **453**, 1091–1094.
- Enfield, D. B., A. M. Mestas-Núñez, and P. J. Trimble, 2001: The Atlantic Multidecadal Oscillation and its relation to rainfall and river flows in the continental U.S. *Geophys. Res. Lett.*, **28**, 2077–2080.
- Evan, A. T., D. J. Vimont, A. K. Heidinger, J. P. Kossin, and R. Bennart, 2009: The role of aerosols in the evolution of tropical North Atlantic Ocean temperature anomalies. *Science*, **324**, 778–781.
- Gleckler, B. D., and Coauthors, 2012: Human-induced global ocean warming on multidecadal timescales. *Nat. Climate Change*, **2**, 524–529, doi:10.1038/nclimate1553.
- Goldenberg, S. B., C. W. Landsea, A. M. Mestas-Núñez, and W. M. Gray, 2001: The recent increase in Atlantic hurricane activity: Causes and implications. *Science*, **293**, 474–479.
- Ishii, M., and M. Kimoto, 2009: Reevaluation of historical ocean heat content variations with time-varying XBT and MBT depth bias corrections. *J. Oceanogr.*, **65**, 287–299.
- Jones, C. D., and Coauthors, 2011: The HadGEM2-ES implementation of CMIP5 centennial simulations. *Geosci. Model Dev.*, **4**, 543–570.
- Knight, J. R., R. J. Allan, C. K. Folland, M. Vellinga, and M. E. Mann, 2005: A signature of persistent natural thermohaline circulation cycles in observed climate. *Geophys. Res. Lett.*, **32**, L20708, doi:10.1029/2005GL024233.
- , C. K. Folland, and A. A. Scaife, 2006: Climate impacts of the Atlantic Multidecadal Oscillation. *Geophys. Res. Lett.*, **33**, L17706, doi:10.1029/2006GL026242.
- Kravtsov, S., and C. Spanngale, 2008: Multidecadal climate variability in observed and modeled surface temperatures. *J. Climate*, **21**, 1104–1121.
- Kushnir, K., and M. Stein, 2010: North Atlantic influence on 19th–20th century rainfall in the Dead Sea watershed, teleconnections with the Sahel, and implication for Holocene climate fluctuations. *Quat. Sci. Rev.*, **29**, 3843–3860, doi:10.1016/j.quascirev.2010.09.004.
- Latif, M., and Coauthors, 2004: Reconstructing, monitoring, and predicting multidecadal-scale changes in the North Atlantic thermohaline circulation with sea surface temperature. *J. Climate*, **17**, 1605–1614.
- Levitus, S., J. I. Antonov, T. P. Boyer, R. A. Locarnini, H. E. Garcia, and A. V. Mishonov, 2009: Global ocean heat content 1955–2008 in light of recently revealed instrumentation problems. *Geophys. Res. Lett.*, **36**, L07608, doi:10.1029/2008GL037155.
- Lohmann, U., and Coauthors, 2010: Total aerosol effect: Radiative forcing or radiative flux perturbation? *Atmos. Chem. Phys.*, **10**, 3235–3246, doi:10.5194/acp-10-3235-2010.
- Mann, M. E., and K. A. Emanuel, 2006: Atlantic hurricane trends linked to climate change. *Eos, Trans. Amer. Geophys. Union*, **87**, 233–241.
- Marshall, J. C., and A. J. G. Nurser, 1992: Fluid dynamics of oceanic thermocline ventilation. *J. Phys. Oceanogr.*, **22**, 583–595.
- Rayner, N. A., D. E. Parker, E. B. Horton, C. K. Folland, L. V. Alexander, D. P. Rowell, E. C. Kent, and A. Kaplan, 2003: Global analyses of sea surface temperature, sea ice, and night marine air temperature since the late nineteenth century. *J. Geophys. Res.*, **108**, 4407, doi:10.1029/2002JD002670.
- Robson, J., R. Sutton, K. Lohmann, D. Smith, and M. D. Palmer, 2012: Causes of the rapid warming of the North Atlantic Ocean in the mid-1990s. *J. Climate*, **25**, 4116–4134.
- Schmidt, M. W., P. Chang, J. E. Hertzberg, T. R. Them, L. Ji, and B. L. Otto-Bliesner, 2012: Impact of abrupt deglacial climate change on tropical Atlantic subsurface temperatures. *Proc. Natl. Acad. Sci. USA*, **109**, 14 348–14 352, doi:10.1073/pnas.1207806109.
- Sutton, R. T., and D. L. R. Hodson, 2005: Atlantic Ocean forcing of North American and European summer climate. *Science*, **309**, 115–118.
- , and B. Dong, 2012: Atlantic Ocean influence on a shift in European climate in the 1990s. *Nat. Geosci.*, **5**, 788–792.
- Terray, L., 2012: Evidence for multiple drivers of North Atlantic multi-decadal climate variability. *Geophys. Res. Lett.*, **39**, L19712, doi:10.1029/2012GL053046.
- Thompson, D. W. J., J. M. Wallace, J. J. Kennedy, and P. D. Jones, 2010: An abrupt drop in Northern Hemisphere sea surface temperature around 1970. *Nature*, **467**, 444–447.
- Ting, M., Y. Kushnir, R. Seager, and C. Li, 2009: Forced and internal twentieth-century SST trends in the North Atlantic. *J. Climate*, **22**, 1469–1481.

- , —, — and L. Cuihua, 2011: Robust features of Atlantic multi-decadal variability and its climate impacts. *Geophys. Res. Lett.*, **38**, L17705, doi:10.1029/2011GL048712.
- Villarini, G., and G. A. Vecchi, 2013: Projected increases in North Atlantic tropical cyclone intensity from CMIP5 models. *J. Climate*, in press.
- Wu, Z., N. E. Huang, J. M. Wallace, B. Smoliak, and X. Chen, 2011: On the time-varying trend in global-mean surface temperature. *Climate Dyn.*, **37**, 759–773, doi:10.1007/s00382-011-1128-8.
- Zhang, R., 2007: Anticorrelated multidecadal variations between surface and subsurface tropical North Atlantic. *Geophys. Res. Lett.*, **34**, L12713, doi:10.1029/2007GL030225.
- , and T. L. Delworth, 2005: Simulated tropical response to a substantial weakening of the Atlantic thermohaline circulation. *J. Climate*, **18**, 1853–1860.
- , and —, 2006: Impact of Atlantic multidecadal oscillations on India/Sahel rainfall and Atlantic hurricanes. *Geophys. Res. Lett.*, **33**, L17712, doi:10.1029/2006GL026267.
- , and —, 2009: A new method for attributing climate variations over the Atlantic Hurricane Basin's main development region. *Geophys. Res. Lett.*, **36**, L06701, doi:10.1029/2009GL037260.
- , —, and I. M. Held, 2007: Can the Atlantic Ocean drive the observed multidecadal variability in Northern Hemisphere mean temperature? *Geophys. Res. Lett.*, **34**, L02709, doi:10.1029/2006GL028683.